

# Identification and Role of Thiols in *Toxoplasma gondii* Egress

ELIJAH W. STOMMEL,\* EUNSUNG CHO,† JEAN ALEX STEIDE,† ROSANNE SEGUIN,‡  
AARON BARCHOWSKY,§ JOSEPH D. SCHWARTZMAN,¶ AND LLOYD H. KASPER\*†

Departments of \*Medicine (Section of Neurology), †Microbiology, §Pharmacology, and ¶Pathology, Dartmouth Medical School, Lebanon, New Hampshire 03756; and ‡Neuroimmunology Unit, Montreal Neurological Institute, 3801 University, Montreal, Quebec H3A 2B4, Canada

The nucleoside triphosphate hydrolase of *Toxoplasma gondii* is a potent apyrase that is secreted into the parasitophorous vacuole where it appears to be essentially inactive in an oxidized form. Recent evidence shows that nucleoside triphosphate hydrolase can be activated by dithiothreitol *in vivo*. On reduction of the enzyme, there is a rapid depletion of host cell ATP. Previous results also demonstrate a dithiothreitol induced egress of parasites from the host cell with a concurrent  $\text{Ca}^{2+}$  flux, postulated to be a consequence of the release of ATP-dependent  $\text{Ca}^{2+}$  stores within the tubulovesicular network of the parasitophorous vacuole. Reduction of the nucleoside triphosphate hydrolase appears crucial for its activation; however, the exact mechanism of reduction/activation has not been determined. Using a variety of techniques, we show here that glutathione promoters activate a  $\text{Ca}^{2+}$  flux and decrease ATP levels in infected human fibroblasts. We further show the *in vitro* activation of nucleoside triphosphate hydrolase by endogenous reducing agents, one of which we postulate might be secreted into the PV by *T. gondii*. Our findings suggest that the reduction of the parasite nucleoside triphosphate hydrolase, and ultimately parasite egress, is under the control of the parasites themselves. [Exp Biol Med Vol. 226(3):229–236, 2001]

**Key words:** *Toxoplasma gondii*;  $\text{Ca}^{2+}$ ; nucleoside triphosphate hydrolase; n-acetyl-cysteine; glutathione; glutathione s-transferase; glutaredoxin; thioredoxin

**T***oxoplasma gondii* is an obligate intracellular parasite that resides within a parasitophorous vacuole (PV). Replication of *T. gondii* within the host cell requires an organized interaction between the host cell and the parasite and involves a number of highly conserved pathways (1). One such interaction is the secretion of nucleoside triphosphate hydrolase (NTPase) by *T. gondii* into the parasitophorous vacuole (PV) (2, 3). The NTPase, when activated

by dithiothreitol (DTT), may trigger parasite egress by reducing host cell ATP levels (4). Egress of the parasites has been shown to depend on a  $\text{Ca}^{2+}$  signal (5) that may come from within the PV (6), or the parasites themselves (7) and may be regulated by intracellular ATP levels (4, 6, 7). Previous studies suggest a sequestration of  $\text{Ca}^{2+}$  within the PV during parasite replication, (8) postulated to be within the tubulo-vesicular network (TVN) within the PV (6). The mechanism of *in vivo* NTPase reduction leading to host cell ATP depletion and subsequent  $\text{Ca}^{2+}$  release and egress is unknown.

DTT and related dithiols, including dithioerythritol (DTE) and to a lesser extent, dimercaptopropanol (MCP), activate NTPases *in vitro*; however, the monothiols 2-mercaptoethanol and glutathione (GSH) have not been shown to activate these enzymes (4, 9) *in vitro* or *in vivo*. In the absence of any dithiol compounds, these enzymes have less than 5% of their *in vitro* activity in the presence of DTT (10). Using GSH promoters, immunohistochemistry, NTPase calorimetric assays and ATP measurements, we provide evidence here for a possible mechanism for reduction/activation of the parasite-derived NTPase.

## Materials and Methods

**Preparation and Infection of Human Fibroblasts.** Human fibroblasts (HF) and the RH strain of *T. gondii* were maintained in tissue culture as described previously (11). Cells were plated on Lab Tek coverslip chambers (NUNC, Naperville, IL) for  $\text{Ca}^{2+}$  imaging experiments. HF ( $= 5 \times 10^4$ ) in modified essential medium-Eagle's (MEM-E)/10% newborn calf serum (NCS) were plated and incubated at (37°C in 5%  $\text{CO}_2$ /95% air). For other experiments we used HF monolayers in 25  $\text{cm}^2$  tissue culture flasks (Corning Costar Corporation, Cambridge, MA). Near confluent HF monolayers were infected with approximately  $(0.5\text{--}2) \times 10^5$  tachyzoites and incubated for an additional 18–36 hr for most experiments.

**Reagents.** Chemicals including DTT, DTE, N-acetylcysteine (NAC), ionomycin, GSH, lipoic acid, glutathione S-transferase, glutathione, ethacrynic acid, and anti-

This work was supported by the National Institutes of Health (NIH A119613 and AI30000).

<sup>1</sup> To whom correspondence should be addressed at Section of Neurology, Dartmouth Hitchcock Medical Center, Lebanon, NH 03756. E-mail: Elijah.W.Stommel@Hitchcock.org

Received June 5, 2000.  
Accepted November 10, 2000.

0037-9727/01/2263-0229\$15.00  
Copyright © 2001 by the Society for Experimental Biology and Medicine

mycin were obtained from Sigma (St. Louis, MO) and diluted in either DMSO, H<sub>2</sub>O or ethanol as stock solutions. With dilution, neither the ethanol nor DMSO had any physiological effect on the cells. Indo-1-AM, monochlorobimane (mBCl) and monobromobimane (mBBr) were obtained from Molecular Probes (Eugene, OR). Glutathione-monoethyl ester (GME) was obtained from Bachem Bioscience (Bubendorf, Switzerland). Secondary antibodies came from Jackson ImmunoResearch Laboratories, Inc. (West Grove, PA) or Amersham Pharmacia Biotech, Inc. (Piscataway, NJ).

Glutaredoxin (GRX) and thioredoxin (TRX) and goat anti-human TRX and goat anti-human GRX all came from American Diagnostica Inc. (Greenwich, CT).

**Ca<sup>2+</sup> Imaging.** Ca<sup>2+</sup> imaging was performed on an Ultima laser, adherent cell analysis system (ACAS), confocal microscope system (Meridian Instruments, Okemos, MI) as previously described (6). HF adhering to coverslip chambers were illuminated with a wavelength of 351/364 nm UV light from an argon ion laser. Using a wide (non-confocal) pinhole aperture, fluorescence from Indo-1-AM was split with a 445-nm long pass dichroic mirror and detected with two photomultiplier tubes (at a wavelength of 405/45 nm and 485/45 nm). Meridian software was used to acquire consecutive images and to plot the changes of this ratio over time. The ratio of fluorescence at 405 nm/485 nm increases as the concentration of Ca<sup>2+</sup> in the medium increases (6). The quantitation of the relationship between the fluorescence ratio and the Ca<sup>2+</sup> concentration can be determined by the Grynkiewicz equation (12); however, we did not attempt to calculate Ca<sup>2+</sup> concentrations in all our experiments. The system allowed visualization with an inverted Olympus microscope using brightfield microscopy when not using fluorescence.

**Determination of Intracellular ATP Levels.** The luciferase/ luciferin assay was used to measure cellular ATP levels (Analytical Luminescence Laboratory, Ann Arbor, MI) in 23-mm dishes. The HF were uninfected, lightly infected (less than 18 hr post-infection and PVs containing fewer than 32 parasites each, with no cell lysis), or heavily infected HF (24–36 hr post-infection where the parasites had begun to lyse some HF and where PVs containing more than 32 parasites were prevalent). Infected HF were exposed to DTT, GSH, NAC, or GME for various lengths of time. The reaction was arrested by washing out the solution with cold phosphate-buffered saline (PBS). The cells were then lysed with 200  $\mu$ l of buffer containing 25mM glycylglycine, 4 mM EGTA, 15 mM MgSO<sub>4</sub>, and 1% Triton X-100. DTT was not included in any of the reaction media but was present in the luciferin reaction medium (1mM) after the cells were lysed. The cells were scraped from the plates, placed into Eppendorf tubes on ice and spun at 13,000 rpm (at 4°C) for 5 min. The supernate was transferred to new tubes for testing with the luciferase/luciferin assay. As a positive control we depleted infected HF of ATP with antimycin (2 mg/ml) and also carried out the above

described experiments with uninfected HF. We used the BCA protein assay (Pierce Chemical Company, Rockford, IL) to normalize ATP measurements with respect to total cellular protein.

**Microscopic GSH Localization.** A heterocyclic bimane dye, mBCl, passively diffuses across the cell membrane into the cytoplasm where it becomes conjugated to the peptide GSH through a reaction with the thiol group (18).

Monobromobimane (mBBr), an analogue to mBCl, was also used in the same manner and concentration as mBCl. MBBr has the benefit of staining human cell lines better than mBCl and the disadvantage of reacting more readily with protein sulfhydryls to give a higher background fluorescence (13). We observed cells stained with these compounds on an inverted Zeiss Axiophot Microscope equipped with a transfluorescence unit, Bio-Rad Confocal imaging system (Hemel Hempstead, UK) and with the ACAS.

**Immunohistochemistry.** HF were grown and infected on Teflon-coated multiwell slides. The monolayers were rinsed with PBS, fixed with 4% paraformaldehyde in PBS with 50 mM K-EGTA (PBS/EGTA) for 5 min at 4°C, washed in PBS/EGTA and treated with the same buffer with 0.1% bovine serum albumin (BSA). The monolayers were permeabilized with 0.10% TX-100 in PBS/EGTA/BSA solution. Tissue preparations were exposed to primary antibody diluted in PBS/EGTA with 0.1% BSA at varying concentrations (1/25, 1/50, 1/100) for 25 min at room temperature. The preparations were then washed in the same buffer, exposed to secondary antibody (1/250 FITC-conjugated goat-anti-rabbit; Vector labs, Burlingame, CA) and then washed. The preparation was mounted with Vectashield (Vector Laboratories, Inc., Burlingame, CA) under glass coverslips. Images were taken using a Bio-Rad confocal imaging system at a wavelength of 488 nm for excitation and a wavelength of 522  $\pm$  16 nm for emission

**NTPase Assays.** NTPase assays were performed on parasites resuspended in lysis buffer (20 mM HEPES, pH 7.5, 20% glycerol, 0.01% Triton X-100) at approximately 10<sup>6</sup>–10<sup>7</sup> parasites/ml. In tubes, 50  $\mu$ l of lysed parasites was mixed with 50  $\mu$ l of ATP substrate [55 mg ATP, 75 mg Mg(CH<sub>3</sub>COO)<sub>2</sub>, and 298 mg HEPES to 25 ml, pH 7.5]. DTT was eliminated from the ATP substrate except in experiments specifically examining its effect. The various thiol reagents were tested by addition to the system at given concentrations. Tubes were incubated for 15 min at 37°C, then 50  $\mu$ l of stop solution (0.1 N HCl) added; 50  $\mu$ l of acid molybdate (Sigma Diagnostics)/Fiske and Subbarow Reducer (SIGMA Diagnostics) [4:1; freshly made] was added to the solution and incubated at RT for 15 min. Adsorption was then read at A<sub>650</sub>.

## Results

**Effects of Thiols on Egress.** The GSH promoters, NAC and GME, were tested for their effects on GSH mediated egress. The redox potential of the PV is likely to regulate the reduction of parasite-derived NTPase that may

deplete host cell ATP (and hence release intra-host cell  $\text{Ca}^{2+}$ ) in a reduced state (4, 6). GSH is poorly permeable to cells (13), and this would explain the lack of response (ATP depletion/egress) observed by Silverman *et al.* (4). Both NAC (1–10 mM) and GME (1–10 mM) which increase intracellular GSH (14, 15), caused parasite egress in larger PV (>32 parasites) in approximately 4–5 min as compared to 1–2 min with DTT (10 mM). The response with the GSH promoters was sometimes delayed for approximately 10–15 min. We observed that larger PVs (>32 parasites/PV) more readily responded to GME or NAC than those PVs containing fewer parasites, but we did not quantitate this observation. Figure 1 demonstrates the response of infected HF to 10 mM NAC. The experiments using NAC and GME were repeated 14 times.

The endogenous reducing agent lipoic acid ( $E^{\circ\prime} -0.288$  V) has a redox potential between DTT ( $E^{\circ\prime} -0.330$  V) and GSH ( $E^{\circ\prime} -0.230$  V) and thus might be another candidate for NTPase activation *in vivo*. We saw no egress response to lipoic acid in concentrations as high as 100  $\mu\text{M}$  (data not shown).

**Effects of NAC on  $\text{Ca}^{2+}$ .** The effect of NAC on  $\text{Ca}^{2+}$  within heavily infected host cells is shown in Fig. 2. A 30% increase in the  $\text{Ca}^{2+}$  ratio was detected in response to 10 mM NAC on *T. gondii*-infected HF as imaged with the

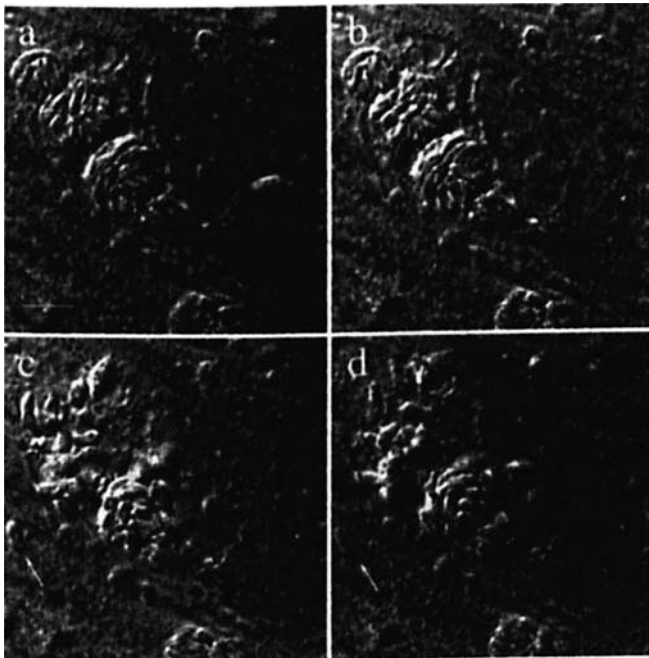


**Figure 1.** Differential interference contrast microscopy showing HF egressing in response to 10mM NAC. There are several extracellular parasites in the medium that are missing from one image to the next as they move out of the field of view. (a) Just before addition of NAC. Horizontal boar represents 10  $\mu\text{m}$ . (b) 4 min after addition of NAC. The parasites have egressed as 6 min. The arrow shows a parasite that just egressed from the uppermost vacuole now penetrating an adjoining HF. The dimpling of this parasite is caused by the constriction of the parasite by the HF membrane. (d) At 8 min this same parasite has now completely entered the HF (arrow). Even after 8 min the PV in the low right-hand corner of the image is still unaffected by NAC. Similar results were obtained using 10mM GME (data not shown).

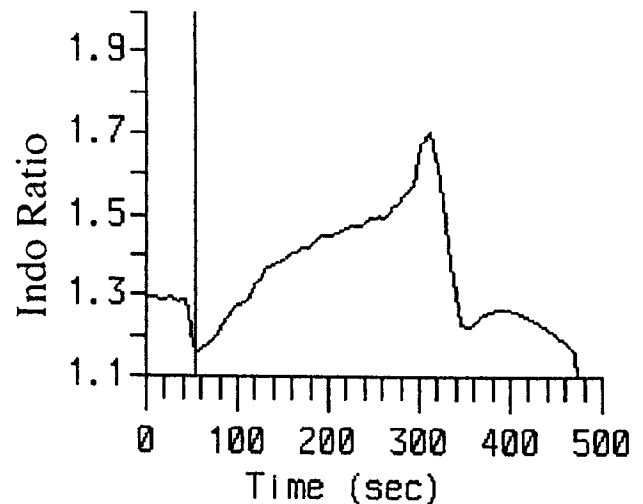


**Figure 2.** ACAS display of ratiometric  $\text{Ca}^{2+}$  measurement using Indo-1-AM stained HF infected with RHEP parasites. NAC (10 mM) was added at 50 sec (vertical bar). A 30% increase in the  $\text{Ca}^{2+}$  ration (y axis) was seen after 4 min at which time the fluorescence was lost as the parasites egressed and the HF lysed.

ACAS with the ratiometric dye Indo-1-AM. The  $\text{Ca}^{2+}$  flux with NAC was not seen in uninfected cells (data not shown).  $\text{Ca}^{2+}$  measurements were not made with GME. Lipoic acid had no effect on the  $\text{Ca}^{2+}$  concentration (data not shown). Figure 2 is a representative example of five experiments, but we did not systematically correlate the magnitude of  $\text{Ca}^{2+}$  release as a function of stage of infection.

**Calculation of ATP Levels.** Figure 3 shows the effects of DTT, NAC, GME, on ATP levels in infected HF. In order to observe the depletion of ATP in response to NAC and GME the HF were heavily infected as evidenced by an abundance of large PVs (32–128 parasites/PV) and visually apparent early host cell lysis. Lightly infected cells that contained no large PVs did not respond to NAC or GME with a drop in ATP. Both NAC and GME generally triggered some increase in ATP levels of uninfected HF (data not shown) and caused depletion of ATP as a function of time in heavily infected HF. As previously reported (6), we saw no effect of extracellular GSH on infected or uninfected HF *in vivo* (data not shown). Figure 3 is a representative example of 12 experiments (11 times in duplicate and one time in quadruplicate). Figure 3 shows ATP levels as % control; however, the ATP levels of infected HF in the presence of NTPase activators was as low as 0.01–0.5 nmol/mg protein compared to 5–10 nmol/mg protein in untreated and uninfected HF as calculated using a standard curve.

**In Vitro NTPase Assays.** *In vitro* NTPase assays were performed in an attempt to define the endogenous thiol responsible for NTPase reduction. As shown in Fig. 4 the endogenous thiols GRX and TRX were found to activate NTPase *in vitro* but not to the same degree as DTT. In contrast to the results of Asai *et al.* (9) there was NTPase activation with GSH as well. Preincubation of TRX and GRX samples with GSH or DTT prior to exposure to parasite samples did not augment the effects of GRX or TRX

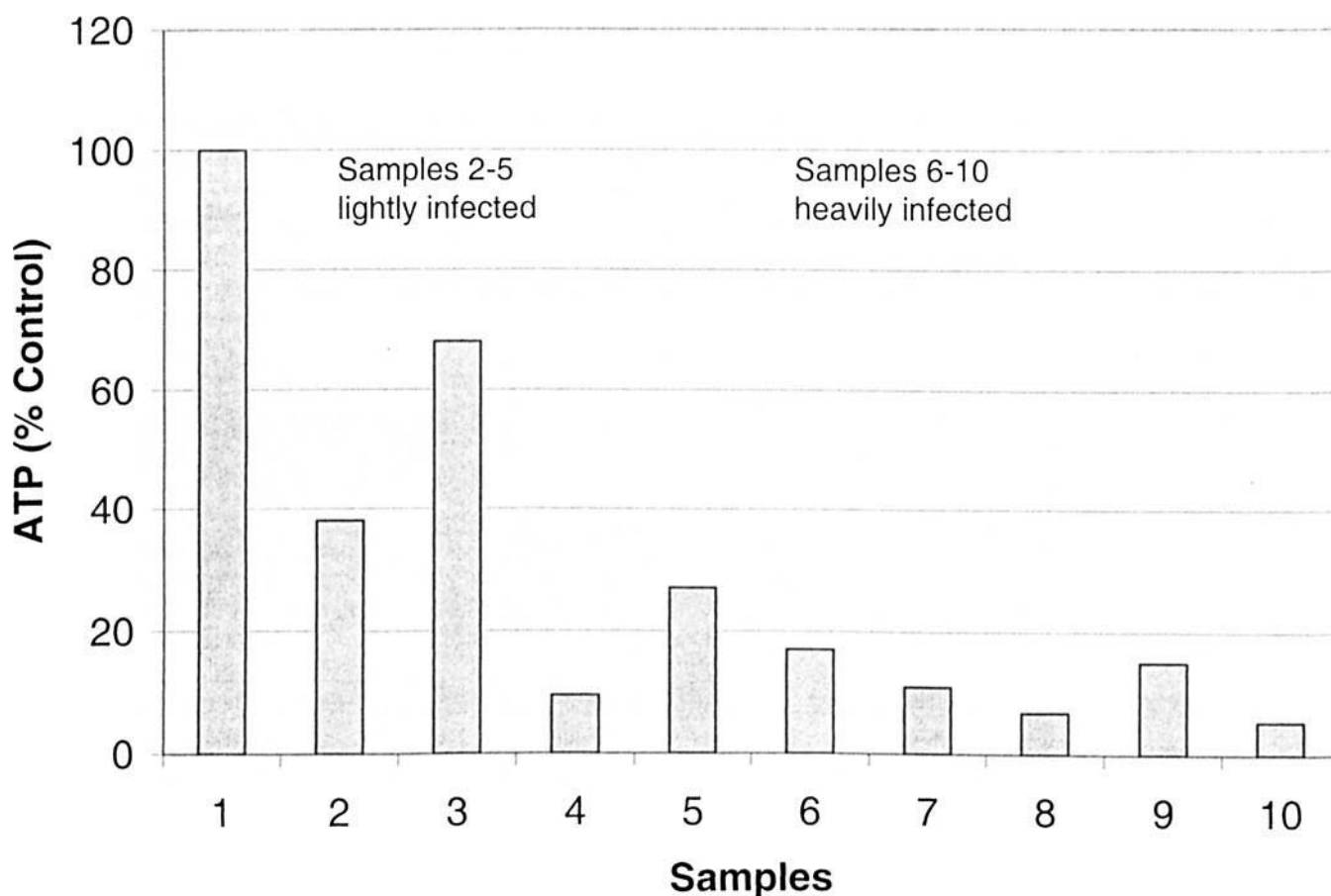


**Figure 3.** Determination of ATP levels in uninfected and infected HF. Rows 2–5 represent infected HF early in infection with PVs containing no more than 8–16 parasites and no evidence of lysis. Rows 6–10 represent infected HF with large PVs (32–128 parasites/PV) and some evidence of HF lysis. Sample 1, uninfected HF; 2, infected HF; 3, infected + 10mM GME for 40 min; 4, infected HF + 10 mM DTT for 10 min; 5, infected HF + 10 mM NAC for 30 min; 6, infected HF; 7, infected HF + 10 mM GME for 10 min; 8, infected HF + 10 mM GME for 40 min; 9, infected HF + 10 mM NAC for 10 min; 10, infected HF + 10 mM NAC for 40 min. Data are representative of one assay. All samples were prepared in duplicate.

(data not shown). GST did not appear to activate NTPase. The assays were performed in duplicate 10 times with DTT at 15 min; 2 times with DTT at 1 min; 7 times with GSH; 10 times with no reagent added; 7 times with TRX; 4 times with GRX; and 4 times with GST. Figure 4 is a compilation of all the experiments for various thiols tested. Using the paired *t*-test, DTT at 15 min was highly significant ( $n = 10$ ;  $P = 0.0064$ ) and GSH less so ( $n = 7$ ;  $P = 0.078$ ) as compared to controls. Using the Student–Newman–Keuls test at  $P < 0.05$  ( $n = 7$ ), DTT was different from controls ( $q = 3.503$ ); GSH was different from controls ( $q = 3.343$ ); but DTT and GSH were not different from each other ( $q = 1.852$ ). The  $n$  values for GRX, TRX, and GST were small for rigorous statistical testing, but were clearly different from DTT, since the DTT values were more than double the controls.

**Bimane Dye Localization with Confocal Microscopy.** Both mBCl and mBBr fluorescence reflect levels of either GSH or GST (16–18). mBCl reflects glutathione *S*-transferase (GST) levels as the later promotes conjugation of mBCl to GSH to produce a fluorescence signal (17). The fluorescence intensity of mBCl was used to localize GSH

with an excitation wavelength of 351–363 nm and emitted fluorescence (461 nm) detected with a barrier filter (BP 485/45 nm). With infected HF stained with mBCl and mBBr, *T. gondii* parasites were substantially brighter than the surrounding cytoplasm of the PV and HF (Fig. 5a,b). As shown in Fig. 5b there appeared to be intra-parasite apical and posterior granules that contained noticeably brighter mBCl staining, suggesting higher levels of either GSH or GST. High-magnification images with the ACAS often demonstrated a gradient of fluorescence intensity from the parasite to the PV to the HF cytoplasm (data not shown). Interestingly, the addition of the mBCl and mBBr often prevented the egress response of the parasites to the NAC and GME. mBCl images represent 12 experiments and mBBr images 6 experiments.

**Immunofluorescence Studies.** Because of the brighter staining of mBCl and mBBr in the parasites compared to the HF, we felt that the levels of GST might be higher within the parasites themselves, thus promoting GSH conjugation to the bimanes, as previously described (19). Immunofluorescence labeling of infected HF with a rabbit GST-antibody revealed parasites that were generally

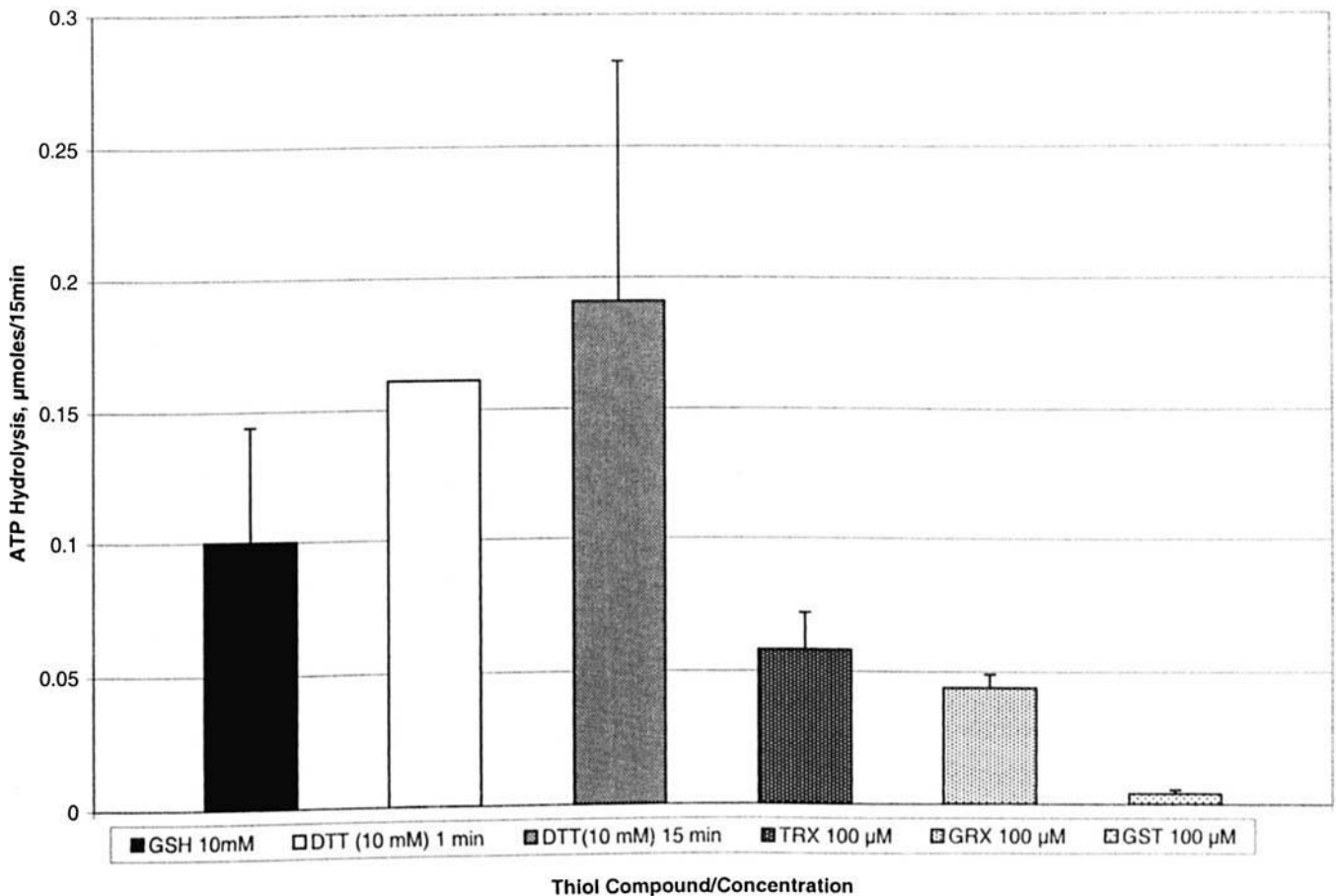


**Figure 4.** *In vitro* NTPase adday of whole parasite extracts. All assays were run in duplicate. The addition of GSH to TRX, GRX, and GST assays had no demonstrable effect (data not shown). ATP hydrolysis for 15 min at 37°C (with the exception of DTT exposure for 1 min) was measured as described in the Materials and Methods. Standard deviations are shown except with DTT (1 min) which represents only two experiments.

brighter than the HF, containing areas of intense staining both at the apex and the posterior pole (Fig. 5c). There were also areas of intense staining suggestive of vacuoles within the cytoplasm of the parasites (Fig. 5c). The distribution of staining showed similarities between GST- and the bimanane dyes (mBCL and mBBr) suggesting that the areas of brightness with the bimanane dyes might reflect higher levels of GST related conjugation of bimanane dyes to thiols.

The intravacuolar space within larger PV (64–128) was often brightly stained with GST antibody so that the boundaries of the PV membrane were well defined (Fig. 5d). This observation was not seen with smaller PV where the parasites stained intensely but the PV was not well defined. Those PV's where the intravacuolar space stained well had parasites that were relatively unstained with GST antibody.

Immunofluorescence labeling was also performed using an anti-GRX and TRX antibody. Staining within the parasites was seen with GRX labeling (Fig. 6); however, there was a lack of staining with the TRX antibody within the PV or parasite (data not shown). With GRX staining, the PV stained brightest along with the outer membrane of the intra-PV parasites. There also appeared to be a slight shift in the distribution of the GRX staining from the parasite to the PV as parasite replication increased. Controls using second-

ary antibody alone or rabbit IgG (50 µg/ml) when staining for GST or with primary exposure to goat serum (50 µg/ml) when staining for GRX, showed no significant staining (Fig. 6g,h). These antibodies did not detect typical GST or GRX bands by western blot. Immuno-electron microscopy experiments did not correlate with the immuno-histochemistry either.

## Discussion

Our results suggest that GSH is in part responsible for NTPase activation *in vivo*. The promoter of intracellular GSH, NAC, is capable of stimulating both a Ca<sup>2+</sup> flux (only in infected HF) and egress similar to that seen with DTT (6). The time required for NAC induction of a Ca<sup>2+</sup> flux is longer than that seen with DTT, as is the time to egress, the time to deplete ATP levels in infected HF, and the relative ineffectiveness of GSH in activating NTPase as compared to DTT. We cannot rule out the possibility that other monothiols might be involved in NTPase activation. It seems unlikely that GME would produce substantial levels of any other intracellular thiol than GSH, as it is simply an esterified form of GSH (permeable to cell membranes) that is de-esterified on entry to the cell body (15). The fact that

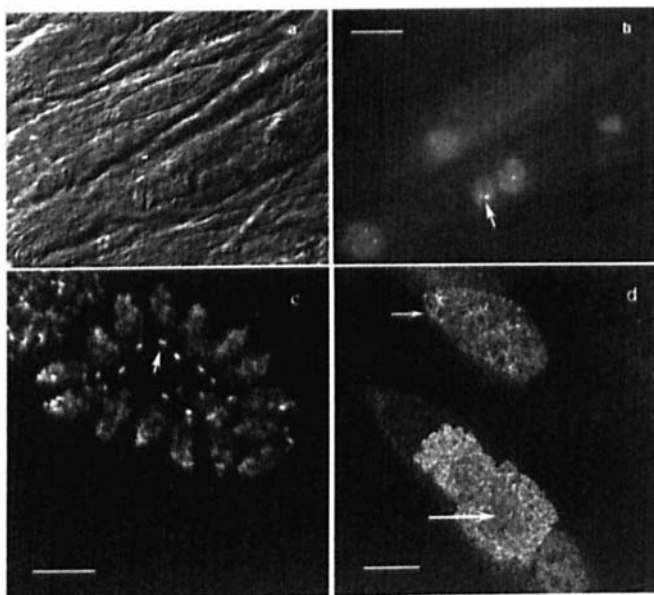


**Figure 5.** Differential interference contrast image of infected HF. (b) Fluorescence image of (a) with mBCl staining. Horizontal bar represents 20  $\mu\text{m}$  for both images a and b. The arrow points out areas of increased fluorescence at the anterior pole of two parasites. (c) Immunolocalization of GST. There was no significant staining with controls using either no primary antibody or non-immune rabbit IgG (50  $\mu\text{g}/\text{ml}$ ) instead of primary antibody (data not shown). The distribution of GST antibody staining is very similar to that seen with bimane staining (mBCl and mBBR). Focal staining is seen at the posterior poles (arrow). Increased staining is also seen anteriorly. Horizontal bar represents 10  $\mu\text{m}$ . (d) GST antibody staining of three large PVs. The upper PV (small arrow) shows a PV with well demarcated borders and poorly stained intra-PV parasites. The poles of these parasites no longer have intense fluorescence. The lower two PVs show intensely stained intra-PV parasites although the lower PV demonstrates some parasites that appear to be losing fluorescence (large arrow) with some increasing fluorescence of the surrounding PV. Horizontal bar represents 10  $\mu\text{m}$ .

extracellular GSH does not activate NTPase *in vivo* (4) can be explained by the fact that GSH is impermeable to cells (13). Asai *et al.* (9) demonstrated no activation of NTPase with GSH *in vitro*. In contrast to our experiments, Asai *et al.* (9) observed the NTPase reactions for 10 min as compared to 15 min and used high-performance liquid chromatography on isolated NTPase instead of the colorimetric assay on whole parasite extracts. Other explanations for this result could be the lack of a critical cofactor lost in the process of NTPase-isolation such as GRX, or the denaturation of the NTPase during purification.

Preincubation of GRX and TRX with DTT or GSH did not change their ability to activate NTPase (data not shown), suggesting that the compounds were already reduced. Addition of GSH to the NTPase assays may simply be reducing a thiol that is necessary for NTPase reduction. GRX gets reduced by GSH and glutathione reductase and has not been shown to be an exclusive substrate of any particular reductase. GST did not substantially activate NTPase in our assays. As the usual role of GST is to make adducts to proteins, and generally not to reduce them (19), GST seems a less likely candidate for NTPase reduction. A more likely

role for GST would be to protect the parasites from toxins and oxidants.

Immunolocalization of GRX and GST suggests that after several rounds of parasite replication these compounds are secreted by parasites into the PV as the parasites lose their fluorescence and the PV become slightly brighter and more delineated. There is no data to suggest that the PV has the ability to transport GRX or GST from the host cell into the PV. Although TRX appears to activate NTPase in our assays and in previous studies (20), available antibodies did not demonstrate its presence. If such an endogenous reducing agent as GRX were necessary as a cofactor for the reduction of NTPase by GSH then dilution or loss of GRX in the process of NTPase isolation might result in loss of GSH-dependent NTPase activation. The PV has pores that allow substances of mol wt <12,000 to pass through (21). *In vivo*, parasite-derived GRX (mol wt 12,000), would be trapped within the PV where it could be markedly more concentrated than *in vitro*. Unfortunately we were unable to obtain reproducible staining with immuno-EM using antibodies to GRX, and thus ultrastructural localization is unclear. Unfortunately, multiple western blotting attempts did not confirm the presence of proteins corresponding to the molecular weights of GST or GRX with the available antibodies. A positive western blot would bolster our immunolocalization results, but the lack of utility of the antibodies for western blotting does not refute them. The monothiols (NAC and GME) preferentially effected NTPase activity and ATP levels late in infection. This may be because GRX needs to be present to facilitate the NTPase reduction by GSH, and that sufficient concentration only occurs late in infection when it is secreted into the PV from the parasites.

The PV environment contains several components that are secreted by the parasites including rhopty proteins, dense granule proteins and NTPase (22). Our data would suggest that the parasite may also secrete a reducing agent, and that this reducing agent may play a role in control of parasite motility. Previous results have shown that the potent *Toxoplasma* NTPase is found largely in an inactive, oxidized form in the PV and readily activated/reduced by DTT with a subsequent rapid depletion of host ATP and egress of parasites (4). The PV environment could be expected to be reduced as it is in equilibrium with the host cytoplasm through the pores in the PV membrane (21). Yet, this reduced environment by itself does not appear to be able to activate the NTPase (4). In fact, infected HF did not show a generalized increase in GSH by mBCL staining with progressive infection. If the environment of the entire host cell determined the reduction of NTPase, then one would expect to see a generalized increase in mBCL staining with progressive infection. GRX, unlike GST, is a reducing agent specifically used to reduce enzymes (19), and it appears to activate the NTPase in our *in vitro* assays, albeit less than DTT. GST (17) enhances the conjugation of mBCl and mBBR to GSH, although there is no evidence that GSH binding is enhanced by GRX. The degree of phosphate pro-

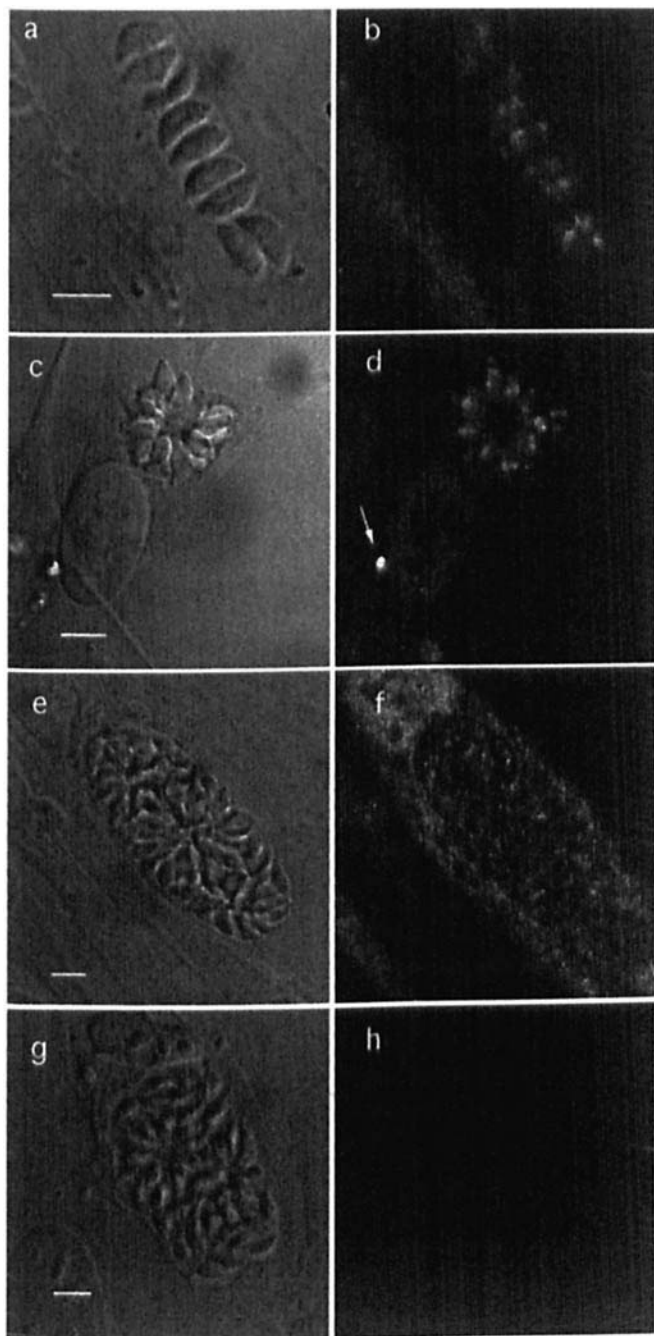


**Figure 6.** Each paired image (left to right) is a differential interference contrast image and immunofluorescence image respectively. Differential interference contrast image of RH parasites in vacuoles. Horizontal bar represents 10  $\mu$ m. (b) Immunolocalization of GRX in same cells. The parasites are brighter than the surrounding cytoplasm of the HF's and areas of discrete staining are seen within the parasites. (c) Differential interference contrast image of small PV. Horizontal bar represents 10  $\mu$ m. (d) Immunolocalization of GRX. Discrete areas of staining are seen within the parasites. The parasites are brighter than the HF. The arrow points to an extracellular parasite that is brighter than anything else in the image. (e) Differential interference contrast image of large PV. Horizontal bar represents 10  $\mu$ m. (f) Immunolocalization of GRX demonstrating a relative reduction in the fluorescence intensity of the parasites compared to the HF and a loss of the discrete areas of increased fluorescence within the parasites. The fluorescence is concentrated within the PV and around the parasite outer membrane. (g) Differential interference contrast image of medium size PV. Horizontal bar represents 10  $\mu$ m. (h) There was no significant staining with controls with either an absence of exposure to primary antibody, as shown here, or initial exposure to goat IgG (50  $\mu$ g/ml).

duction in 15 min with GSH and GRX appears similar to that produced by DTT in 1 min. At 1 min DTT gave a value of 77% of the corresponding 15 min determination, reflecting the remarkable effect of DTT on NTPase activation. DTT is a vicinal dithiol and its structure gives it a markedly different reactivity than monothiols like NAC or GSH (23). In fact, some effects can be discriminated by whether they are enhanced by mono or dithiols (24). DTT is a stronger reductant than GSH because the vicinal dithiol is more spontaneously reactive (23). Furthermore, its ability to activate NTPase does not appear to require a cofactor.

With the GSH promoters, NAC and GME, one would expect the levels of GSH to increase dramatically over a relatively short time period, based on the time required for  $\text{Ca}^{2+}$  flux and parasite egress in response to these reagents. Unfortunately, we were unable to monitor the accumulation of GSH with mBCl over long time periods because of photobleaching. Continuous secretion of GRX or GST into the PV would have the effect of increasing the concentration of reducing factors, just where NTPase is secreted (12), and suggests the possible parasite regulation of NTPase activation. From a biochemical perspective, elevations in GSH would favor the activation of NTPase (as shown in luciferase/luciferin assays) as the excess of GSH would favor the reduction of intra-PV GRX. The fact that mBCl generally inhibits the egress of parasites exposed to GME or NAC may be explained by the fact that the dye would effectively diminish the amount of active intracellular GSH by binding to the sulhydryl moieties. If secretion of GRX is indeed responsible for the ultimate reduction of NTPase, then it will be important to investigate the control of secretion of this thiol.

Image cytometry was done at Dartmouth Medical School in The Herbert C. Englert Cell Analysis Laboratory, which was established by a grant from the Fannie E. Rippel Foundation and is supported in part by a Core Grant of the Norris Cotton Cancer Center (CA 23108). We thank Kenneth Orndorff for his expertise using various imaging techniques and Dr. Matthew Heintzelman for his assistance with biochemical and histological techniques.

1. Smith JE. A ubiquitous intracellular parasite: The cellular biology of *Toxoplasma gondii*. *Internat J Parasitol* **25**:1301–1309, 1995.
2. Sibley LD, Niesman IR, Asai T, Takeuchi T. *Toxoplasma gondii*: secretion of a potent nucleoside triphosphate hydrolase into the parasitophorous vacuole. *Exp Parasitol* **79**:301–311, 1994.
3. Bermudes D, Peck KR, Afifi MA, Beckers CJ, Joiner KA. Tandemly repeated genes encode nucleoside triphosphate hydrolase isoforms secreted into the parasitophorous vacuole of *Toxoplasma gondii*. *J Biol Chem* **269**:29252–29260, 1994.
4. Silverman JA, Qi H, Riehl A, Beckers C, Nakaar V, Joiner KA. Induced activation of the *Toxoplasma gondii* nucleoside triphosphate hydrolase leads to depletion of host cell ATP levels and rapid exit of intracellular parasites from infected cells. *J Biol Chem* **273**:12352–12359, 1998.
5. Endo T, Sethi KK, Piekarski G. *Toxoplasma gondii*: Calcium ionophore A23187-mediated exit of trophozoites from infected murine macrophages. *Exp Parasitol* **53**:179–188, 1982.

6. Stommel EW, Ely KH, Schwartzman JD, Kasper LH. *Toxoplasma gondii*: Dithiol-induced  $\text{Ca}^{2+}$  flux causes egress of parasites from the parasitophorous vacuole. *Exp Parasitol* **87**:88–97, 1997.
7. Bouchot A, Zierold K, Bonhomme A, Kilian L, Belloni A, Balossier G, Pinon J, Bonhomme P. Tachyzoite calcium changes during cell invasion by *Toxoplasma gondii*. *Parasitol Res* **85**:809–818, 1999.
8. Pingret L, Millot J, Shanronov S, Bonhomme A, Manfait M, Pinon J. Relationship between intracellular free calcium concentrations and the intracellular development of *Toxoplasma gondii*. *J Histochem Cytochem* **44**:1123–1129, 1996.
9. Asai T, O'Sullivan WJ, Tatibana M. A potent nucleoside triphosphate hydrolase from the parasitic protozoan *T. gondii*. Purification, some properties, and activation by thiol compounds. *J Biol Chem* **258**:6816–6822, 1983.
10. Asai T, Miura S, Sibley LD, Okabayashi H, Takeuchi T. Biochemical and molecular characterization of nucleoside triphosphate hydrolase isozymes from the parasitic protozoan *T. gondii*. *J Biol Chem* **270**:11391–11397, 1995.
11. Joiner KA, Fuhrman SA, Miettinen HM, Kasper LH, Mellman I. *Toxoplasma gondii*: fusion competence of parasitophorous vacuoles in Fc receptor-transfected fibroblasts. *Science* **249**:641–646, 1990.
12. Grynkiewicz G, Poenie M, Tsien RY. A new generation of  $\text{Ca}^{2+}$  indicators with greatly improved fluorescence properties. *J Biol Chem* **260**:3440–3450, 1985.
13. Deneke S M, Fanburg BL. Regulation of cellular glutathione. *Am J Physiol* **257**:L163–L173, 1989.
14. Cotgreave I, Moldeus P, Schuppe I. The metabolism of N-acetylcysteine by human endothelial cells. *Biochem Pharmacol* **42**:13, 1991.
15. Anderson ME, Powrie F, Puri RN, Meister A. Glutathione monoethyl ester: Preparation, uptake by tissues, and conversion to glutathione. *Arch Biochem Biophys* **239**:538–548, 1985.
16. Radkowsky AE, Kosower EM. Bimanes 17. (Haloalkyl)-1,5-diazabicyclo[3.3.0]heptadienediones (halo-9,10-dioxabimanes); Reactivity toward the tripeptide thiol, glutathione. *J Am Chem Soc* **108**:4527–4531, 1986.
17. Barhoumi R, Bailey RH, Burghardt RC. Kinetic analysis of glutathione in anchored cells with monochlorobimane. *Cytometry* **19**:226–234, 1995.
18. Hedley DW, Chow S. Evaluation of methods for measuring cellular glutathione content using flow cytometry. *Cytometry* **15**:349–358, 1994.
19. Bjornstedt M, Kumar S, Bjorkhem L, Spyrou, G, Holmgren A. Selenium and the thioredoxin and glutaredoxin systems. *Biomed Environ Sci* **10**:271–279, 1997.
20. Asai T, Kim T. Possible regulation mechanism of potent nucleoside triphosphate hydrolase in *Toxoplasma gondii*. *ZBI Bakt Hyg A* **264**:464–467, 1987.
21. Schwab JC, Beckers CJ, Joiner KA, Schwartzman JD, Saffer LD. The parasitophorous vacuole membrane surrounding intracellular *Toxoplasma gondii* functions as a molecular sieve. *Proc Natl Acad Sci U S A* **91**:509–513, 1994.
22. Carruthers VB, Sibley LD. Sequential protein secretion from three distinct organelles of *Toxoplasma gondii* accompanies invasion of human fibroblasts. *Eur J Cell Biol* **73**:114–123, 1997.
23. Zahler WL, Cleland WW. A specific and sensitive assay for disulfides. *J Biol Chem* **243**:716–719, 1968.
24. Spiegel AM, Brown EM, Aurbach GD. Inhibition of adenylate cyclase by arsenite and cadmium: Evidence for a vicinal dithiol requirement. *J Cyclic Nucleotide Res* **2**:393–404, 1976.